Spectral-amplitude-encoding optical-code-division-multiplexing system with a heterodyne detection receiver for broadband optical multiple-access networks

Anh T. Pham

The University of Aizu, Aizu-Wakamatsu city, Fukushima 965-8580, Japan

Noriki Miki

NTT Access Network Service System Laboratories, 1-6 Nakase, Mihama-ku, Chiba 261-0023, Japan

Hiroyuki Yashima

Tokyo University of Science, 1-3 Kagurazaka, Shinjuku-ku, Tokyo 162-8601, Japan

pham@u-aizu.ac.jp

RECEIVED 1 JUNE 2005; REVISED 29 JULY 2005;
ACCEPTED 29 JULY 2005; PUBLISHED 7 SEPTEMBER 2005

We propose a spectral-amplitude-encoding optical-code-division-multiplexing (SAE/OCDM) system with a heterodyne detection receiver for broadband optical multiple-access networks (OMANs). The performance of the proposed system is theoretically analyzed, taking into account various types of noise and interference, including multiple-access interference (MAI), cross talk, optical beating interference (OBI), and receiver noise. Analytical results show that the proposed system offers significant improvement in terms of receiver sensitivity and system capacity (number of users) compared with conventional direct-detection systems. We also discuss conditions necessary for a heterodyne detection receiver to work properly in a SAE/OCDM system. In addition, the system performance is analyzed with several signature code sets including *m*-sequence, Hadamard, and modified quadratic congruence (MQC) code sets. It is found that signature code sets with higher weight, such as *m*-sequence and Hadamard code sets, are preferred in a SAE/OCDM system with a heterodyne detection receiver.

OCIS codes: 060.0060, 060.4230, 060.2360.

1. Introduction

The rapid growth of the Internet, broadband services, and Web content in recent years has promoted the presence of optical fiber in last-mile access networks. In optical access networks, multiplexing more than one user on a single optical fiber is desired to reduce cost and to make use of the optical fiber's vast bandwidth. This kind of network is called an optical multiple-access network (OMAN). Current OMANs are deployed on passive optical networks (PONs) and use time division multiplexing (TDM) for the physical layer. However, due to the nature of time multiplexing, the total throughput of a TDM-based system is limited by the electronic processing, which is about 10 Gbits/s. Because demand for ultra-high-speed connections (Gbits/s per user) is expected to appear in the near future, the study of novel multiplexing techniques for the physical layer is attracting much attention from many researchers. Wavelength division multiplexing (WDM) appears to be an attractive technique that can accommodate hundreds of ultra-high-speed users by assigning

them different wavelengths. However, the deployment of WDM in the access environment is still limited because it requires expensive components. Therefore, optical code division multiplexing (OCDM) has emerged as a promising candidate. OCDM is a multiplexing technique that uses an approach different from TDM and WDM. In OCDM systems, the optical fiber's resources (i.e., wavelength and time) are not shared among users; instead all resources are assigned to all users. Multiplexing is achieved by use of signature-encoded signals. OCDM's advantages include ultra-high-speed connections, asynchronous access, scalability, security, and a potentially lower cost than WDM.

OCDM signals can be encoded in either the time or the frequency domain. Time domain encoding is not suitable for a broadband OMAN because of its spectral inefficiency. In frequency domain encoding, a signal can be encoded by using either its spectral amplitude or phase. In both systems, frequency components from a broadband optical source are first resolved. In a spectral-phase-encoding (SPE) system, a SPE grid is employed to apply different phase shifts at various spatially resolved spectral components [1, 2]. In a spectral-amplitude-encoding (SAE) system, a signal is encoded by selectively blocking or transmitting certain frequency components [3–6]. Compared to SPE/OCDM, a SAE/OCDM system is less expensive because it does not require a coherent optical source. For the access environment, where cost is one of the most decisive factors, the SAE/OCDM is therefore regarded to be a more promising candidate.

In frequency-domain-encoding OCDM systems, optical beating interference (OBI), which occurs when a photodetector simultaneously receives two or more optical waves with nearly the same wavelength, occurs due to the use of a broadband optical source. It has been shown that the effect of OBI on system performance is critical [7, 8]. As a matter of fact, when the direct-detection scheme is used with either a noncoherent [7, 9, 10] or a coherent source [8], the number of users in the SAE/OCDM system is severely decreased by OBI; e.g., fewer than 10×1 Gbits/s users can be supported even at a relatively high received optical power of -20 dBm [9]. This makes SAE/OCDM less competitive than WDM, especially in a PON-based access network environment where link loss up to 30 dB is expected [11].

In this paper, we therefore propose to use a heterodyne detection receiver for a SAE/OCDM system to combat OBI and to improve receiver sensitivity. It is well known that the use of a locally generated optical signal (LO) in the heterodyne receiver could improve the receiver's sensitivity up to 20 dB compared with direct-detection systems [12]. In the following sections, we will explore other advantages of using a LO to suppress OBI and consequently to increase the number of users in the SAE/OCDM system. We will discuss the conditions necessary for the heterodyne detection receiver to work efficiently. In addition, we will theoretically analyze the proposed system's performance with various signature code sets and determine which is suitable.

The rest of this paper is organized as follows. Section 2 briefly describes the basic principle of the SAE/OCDM system and its signature code sets. In Section 3, an analytical model of the proposed SAE/OCDM system with a heterodyne detection receiver is proposed and described. Also in Section 3, the bit error rate (BER) of the proposed system is theoretically derived considering various types of noise and interference. Numerical results are presented in Section 4, and Section 5 concludes the paper.

2. Basic Principle of a SAE/OCDM System

The SAE/OCDM technique was first described by Zaccarin and Kavehrad [3]. Figure 1 shows the principle structure of a SAE/OCDM system. At the spectral amplitude encoder, frequency components from a broadband optical source are resolved and encoded by selectively blocking or transmitting certain frequency components in accordance with a signature code. The receiver filters the incoming signal with the same filter [direct decoder,

$A(\omega)$] used at the transmitter as well as its complementary filter [complementary decoder, $\overline{A}(\omega)$]. The outputs from these decoders are detected by two photodetectors connected in a balanced fashion. For an interfering signal, depending on the signature code used, a part of its spectral components will match the direct decoder, and the other part will match the complementary decoder. Since the output of the balanced receiver represents the difference between the two photodetector outputs, the interfering channels will be canceled, whereas the matched channel is demodulated; i.e., multiple-access interference (MAI) is canceled in the SAE/OCDM system.

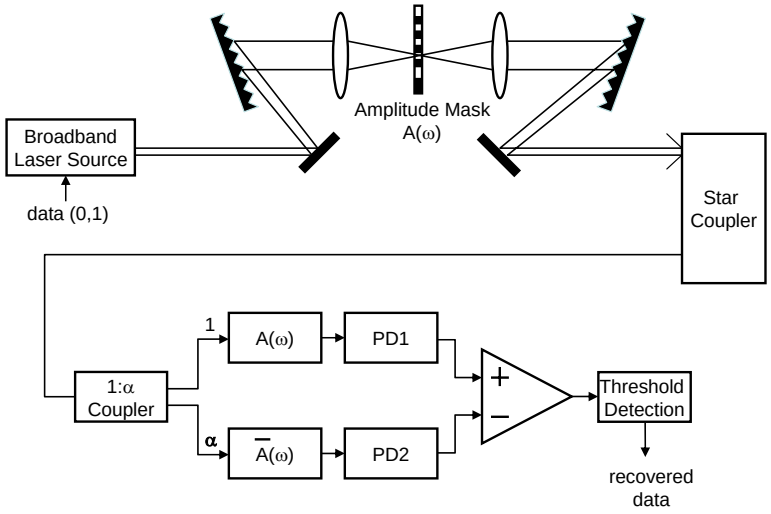

Fig. 1. Principle diagram of a SAE/OCDM system.

Several signature code sets have been proposed for a SAE/OCDM system, including *m*-sequence, Hadamard, and modified quadratic congruence (MQC) code sets [3, 9, 10]. Each of these signature code sets can be represented by its length, weight, and in-phase cross correlation (N,β,γ). In the *m*-sequence code set, $\beta = N+1/2$ and $\gamma = N+1/4$; the weight and in-phase cross correlation of the Hadamard code set are $N/2$ and $N/4$, respectively. In MQC code, $\gamma = 1$, and for an odd prime p, we have code length $N = p^2 + p$ and weight $\beta = p+1$. Constructions of these codes can be found in Refs. [3, 9, 10].

Let $\mathbf{c_d} = [c_d(0), c_d(1), \ldots, c_d(N-1)]$ and $\mathbf{c_k} = [c_k(0), c_k(1), \ldots, c_k(N-1)]$ be two (0,1) signature codes, then the correlation properties are given by

$$\Theta_{\mathbf{c_d},\mathbf{c_k}} = \sum_{i=0}^{N-1} c_d(i)\, c_k(i) = \begin{cases} \beta & \text{if } d = k \\ \gamma & \text{if } d \neq k \end{cases}. \tag{1}$$

The correlation between $\bar{c}_d$ (a complementary of $\mathbf{c_d}$) and $\mathbf{c_k}$ is

$$\Theta_{\bar{\mathbf{c}}_\mathbf{d},\mathbf{c_k}} = \sum_{i=0}^{N-1} \bar{c}_d(i)\, c_k(i) = \beta - \Theta_{\mathbf{c_d},\mathbf{c_k}} = \begin{cases} 0 & \text{if } \mathbf{d} = \mathbf{k} \\ \beta - \gamma & \text{if } \mathbf{d} \neq k \end{cases}. \tag{2}$$

To completely cancel MAI, it is necessary to set a ratio between the optical powers that arrive at the two photodetectors [3, 10] $\alpha = \gamma/\beta - \gamma$. The cancellation of the interfering signal (when $k \neq d$) by the balanced receiver thus can be seen as

$$\Theta_{\mathbf{c_d},\mathbf{c_k}} - \alpha\Theta_{\bar{\mathbf{c}}_\mathbf{d},\mathbf{c_k}} = \gamma - \frac{\gamma}{\beta-\gamma}(\beta-\gamma) = 0. \tag{3}$$

Results from previous research show that a low-weight code, e.g., MQC, is preferable to a high-weight code when OBI is considered, especially when the received optical power is high. In fact, a lower code weight results in a lower signal-to-noise ratio (SNR) if OBI is negligible. This happens in the MQC coded system when the received optical power is low because this optical power is further reduced by a ratio of α in one of the branches. However, when the received optical power is increased, OBI is increased and becomes ineligible. In this case, compared to an *m*-sequence or Hadamard coded system, a MQC coded system has a higher SNR (i.e., better performance) thanks to its low in-phase cross correlation, i.e., resulting in lower OBI (see Fig. 2) [10].

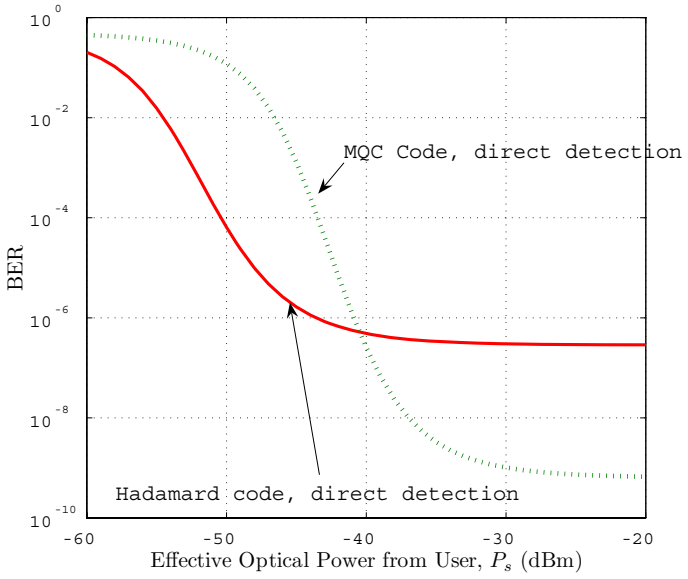

Fig. 2. BER versus effective received power (dBm). Hadamard code (56, 28, 14) versus MQC (56, 8, 1). Direct detection, $P_s = -20$ dBm; number of users, $N = 32 \times 100$ Mbit/s users.

3. Heterodyne Detection SAE/OCDM System

In this section, we present an analytical model of the SAE/OCDM with a heterodyne detection receiver. We then theoretically analyze the system performance by deriving the system's BER using this model.

Figure 3 shows the analytical model of a transmitter–receiver pair in the SAE/OCDM system with a heterodyne detection receiver. At the transmitter, data-carried noncoherent optical pulses from a flattened multicarrier laser source with *N* components are encoded at the spectral encoder before they are transmitted into an optical fiber. This kind of multicarrier source can be achieved based on the pulse compression through fiber nonlinearity that was reported in Refs. [13, 14]. In our analysis, for the case of interest (i.e., a system that supports up to 10 Gbit/s connections), we assume that the multicarrier source with 56 channels and an optical bandwidth of 1.28 THz has an unpolarized and ideally flat spectrum over the bandwidth (i.e., the space between channels $\Delta\omega > 20$ GHz; the reason for this assumption will be explained later in this section).

At the heterodyne detection receiver, the received signal (including MAI) is first mixed coherently with a LO, which is also a multicarrier source that has the same characteristic

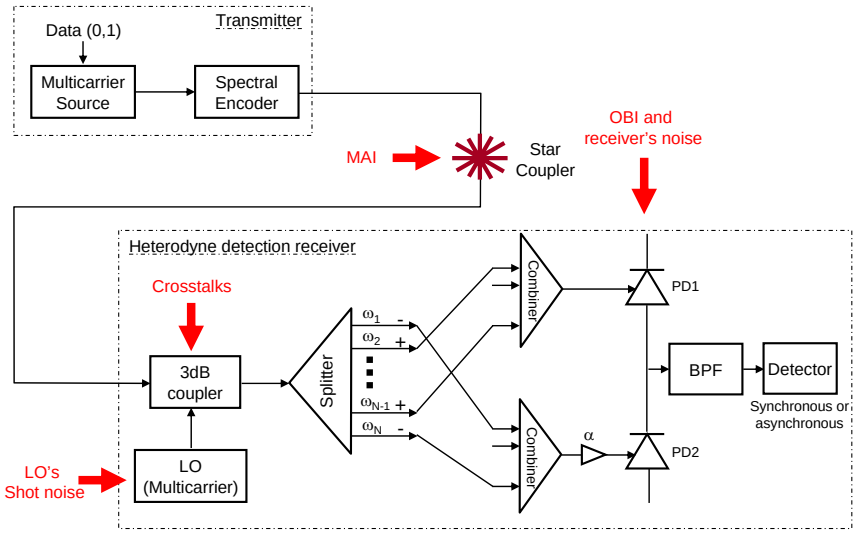

Fig. 3. Analytical model of a transmitter–receiver pair of a proposed heterodyne detection SAE/OCDM system.

as the transmitter. To model the function of direct and complementary decoders, frequency components are split, then signed in accordance with the receiver's signature code, i.e., positive or negative sign for the frequency component that corresponds to chip 1 or chip 0, respectively. Positive- and negative-signed frequency components are combined into two separate branches. The combined signals are then incident on two photodetectors connected in a balanced fashion. Afterward, an electrical signal is passed to a bandpass filter (BPF). The electrical signal is then detected synchronously or asynchronously; we have synchronous and asynchronous heterodyne detection receivers. The asynchronous heterodyne detection receiver is known to be simpler and preferable to the synchronous one, which requires recovery of the microwave carrier at the IF frequency [12]. We will consider both types of detection in this paper.

Let $\omega_{LO}, \varphi_{LO}$ be the frequency and phase of the LO, respectively, then the optical field associated with the LO can be written as

$$E_{LO}(t) \propto \sqrt{P_{LO}} \sum_{i=0}^{N-1} \cos\left[(\omega_{LO} + i\Delta\omega)t + \varphi_{LO}\right], \tag{4}$$

where P_{LO} is the effective power of the LO; $\Delta\omega$ is the space between frequency components, which is assumed to be the same for both the LO and the users; and N is the length of the signature code, i.e., the number of frequency components. Denote $\omega_d, \omega_k, \varphi_d$, and φ_k as frequencies and phases of the desired and kth active users, then the received optical field with K interfering users can be expressed as

$$\begin{aligned} E_s(t) \propto & \underbrace{\sqrt{P_d} \sum_{i=0}^{N-1} c_d(i) \cos[(\omega_d + i\Delta\omega)t + \phi_d]}_{\text{Data}} \\ & + \underbrace{\sum_{k=1}^{K} \sqrt{P_k} \sum_{i=0}^{N-1} c_k(i) \cos[(\omega_k + i\Delta\omega)t + \phi_k]}_{\text{MAI}}, \end{aligned} \tag{5}$$

where P_d and P_k ($P_d = P_k = P_s/N$) are the optical powers per spectral slice from the desired and kth users (for $k \in \{1,\ldots,K\}$), respectively. In our analysis, we assume an identical spectral width for all power spectral components and the same effective power level, P_s, for each user.

Figure 4(a) shows the optical spectra of the LO, as well as the signal from desired user d and interfering user k. In this figure, the dc term in the detector current is filtered out and ignored because $P_{LO} \gg P_d, P_k$. Assuming that bit streams from all users are to be synchronized (the worst case), polarization between the optical signals and the LO are matched, and the photocurrents on the additive branch $I^+(t)$ can be derived as

$$
\begin{aligned}
I^+(t)/\Re = & \underbrace{2\sqrt{P_{LO}P_d}\sum_{i=0}^{N-1} c_d(i)c_d(i)\cos(\omega_{IF_d}t+\Delta\phi_{IF_d})}_{\text{Data:}I^+_{Data}(t)} \\
& + \underbrace{2\sum_{k=1}^{K}\sqrt{P_{LO}P_k}\sum_{i=0}^{N-1} c_d(i)c_k(i)\cos(\omega_{IF_k}t+\Delta\phi_{IF_k})}_{\text{MAI:}I^+_{MAI}(t)} \\
& + \underbrace{2\sqrt{P_{LO}P_d}\sum_{j=0}^{N-1}\sum_{i=0}^{N-1} c_d(i)c_d(i-j)\cos[(\omega_{IF_d}+(i-j)\Delta\omega)t+\Delta\phi_{IF_d}]}_{\text{Self-crosstalk:}I^+_{Data-Cross}(t)} \\
& + \underbrace{2\sum_{k=1}^{K}\sqrt{P_{LO}P_d}\sum_{j=0}^{N-1}\sum_{i=0}^{N-1} c_d(i)c_k(i-j)\cos[(\omega_{IF_k}+(i-j)\Delta\omega)t+\Delta\phi_{IF_k}]}_{\text{MAI-crosstalk:}I^+_{MAI-Cross}(t)} \\
& + \underbrace{2\sum_{k=1}^{K}\sqrt{P_dP_k}\sum_{i=0}^{N-1} c_d(i)\sum_{i=0}^{N-1} c_k(i)\cos(\Delta\omega_{d,k}t+\Delta\phi_{d,k})}_{\text{Primary OBI:}I^+_{OBI1}(t)} \\
& + \underbrace{2\sum_{m=k+1}^{K}\sum_{k=1}^{K-1}\sqrt{P_kP_m}\sum_{i=0}^{N-1} c_d(i)\sum_{i=0}^{N-1} c_k(i)c_m(i)\cos(\Delta\omega_{k,m}t+\Delta\phi_{k,m})}_{\text{Secondary OBI:}I^+_{OBI2}(t)} \\
& + \underbrace{n(t)}_{\text{Receiver's noise}} \quad ,
\end{aligned}
\tag{6}
$$

where $\Re$ is the photodetector responsivity, $\omega_{IF_x} = \omega_x - \omega_{LO}$, $\Delta\omega_{x,y} = \omega_x - \omega_y$, $\Delta\varphi_{x,y} = \varphi_x - \varphi_y$, and $[(x,y) = (d,k,m)]$. The photocurrent on the subtractive branch $I^-(t)$ can also be derived similarly as Eq. (7) below, where $c_d(i)$ is replaced by $\overline{c_d}(i)$ and notations of $I^+_{\text{Data}}(t)$, $I^+_{MAI}(t)$, $I^+_{\text{Data-Cross}}(t)$, $I^+_{MAI\text{-Cross}}(t)$, $I^+_{OBI1}(t)$, and $I^+_{OBI2}(t)$ are replaced by $I^-_{\text{Data}}(t)$, $I^-_{MAI}(t)$, $I^-_{\text{Data-Cross}}(t)$, $I^-_{MAI\text{-Cross}}(t)$, $I^-_{OBI1}(t)$, and $I^-_{OBI2}(t)$, respectively. In addition, it is noted that the signal power in the negative branch is reduced by a ratio of α. The data signal photocurrents then can be derived as

$$
I_{\text{Data}}(t) = I^+_{\text{Data}}(t) - I^-_{\text{Data}}(t) = 2\Re\sqrt{P_{LO}\frac{P_s}{N}}\beta\cos\left(\omega_{IF_d}t+\Delta\varphi_{IF_d}\right). \tag{7}
$$

It is easy to realize that MAI is canceled by the balanced receiver because

$$\begin{aligned} I_{MAI}(t) &= I^{+}_{MAI}(t) - I^{-}_{MAI}(t) \\ &= 2\sum_{k=1}^{K}\sqrt{P_{LO}P_k}\sum_{i=1}^{N} c_d(i)\,c_k(i)\cos\left(\omega_{IF_i}t + \Delta\varphi_{IF_i}\right) \\ &\quad - 2\alpha\sum_{k=1}^{K}\sqrt{P_{LO}P_k}\sum_{i=1}^{N} \bar{c}_d(i)\,c_k(i)\cos\left(\omega_{IF_i}t + \Delta\varphi_{IF_i}\right) \\ &= 0. \end{aligned} \tag{8}$$

OBI, self-cross-talk, and MAI cross talk, however, are not canceled in the balanced receiver because the signals in the two branches of the photodetectors in the SAE/OCDM system are different complementary spectral components. These signals are uncorrelated and added in the detector output. However, as is seen in Fig. 4(b), self-cross-talk and MAI cross talk can be filtered out by the BPF placed after photodetectors provided that $\Delta\omega \geq 2B$, where B is the electrical bandwidth of the photodetector (this condition is satisfied in our previous assumptions; for $B = 10\,\text{GHz}$, an optical bandwidth of 1.28 THz is used with signature codes of 56 chip length).

Total noise variance is thus given by

$$I^2_{\text{Noise}} = I^2_{OBI} + I^2_T + I^2_S, \tag{9}$$

where the first term is the photocurrent caused by OBI and the second and the third terms are the photocurrents caused by the receiver's thermal noise and shot noise, respectively. When all users are sending bit 1, the average power signal and average OBI power, after simplification, are expressed as

$$I^2_{\text{Data}} = 2\Re^2 P_{LO}\frac{P_s}{N}\beta, \tag{10}$$

$$\begin{aligned} I^2_{OBI} &= B\tau_c\left(I^{+}_{OBI1}{}^2 + I^{-}_{OBI1}{}^2 + I^{+}_{OBI2}{}^2 + I^{-}_{OBI2}{}^2\right) \\ &= 2B\tau_c\Re^2\frac{P_s^2}{N^2}\beta K\left[\beta + (K-1)\gamma + (K-1)\frac{\gamma^2}{\beta-\gamma}\right], \end{aligned} \tag{11}$$

where τ_c is the coherence time of the source and $\tau_c \approx 1/B_{opt}$ (B_{opt} is the optical bandwidth of the system). The receiver noises are $I^2_T = 4K_bT_nB/R_L$ and $I^2_S \approx 2eBRP_{LO}$, where K_b is Boltzman's constant, T_n is the receiver temperature noise, R_L is the receiver load resistor, and B is the receiver's electrical bandwidth. When an asymmetric binary channel is assumed, the total noise power can then be derived as

$$I^2_{\text{Noise}} = 4K_bT_nB/R_L + 2eB\Re P_{LO} + B\tau_c\Re^2\frac{P_s^2}{N^2}\beta K\left[\beta + (K-1)\gamma + (K-1)\frac{\gamma^2}{\beta-\gamma}\right]. \tag{12}$$

The SNR hence can be determined as

$$\text{SNR} = \frac{I^2_{\text{Data}}}{I^2_{\text{Noise}}}. \tag{13}$$

Because a bipolar signal can be used in the system using Hadamard or m-sequence code [2, 3], the BER for a synchronous heterodyne detection system can be derived as $\text{BER} = \frac{1}{2}\,\text{erfc}\left(\sqrt{\text{SNR}/2}\right)$. When asynchronous heterodyne detection is used, $\text{BER} = \frac{1}{2}\exp(-\text{SNR}/2)$. In a SAE/OCDM system using MQC code, $\text{BER} = \frac{1}{2}\,\text{erfc}\left(\sqrt{\text{SNR}/8}\right)$ and $\text{BER} = \frac{1}{2}\exp(-\text{SNR}/8)$ for synchronous and asynchronous heterodyne detection, respectively [15].

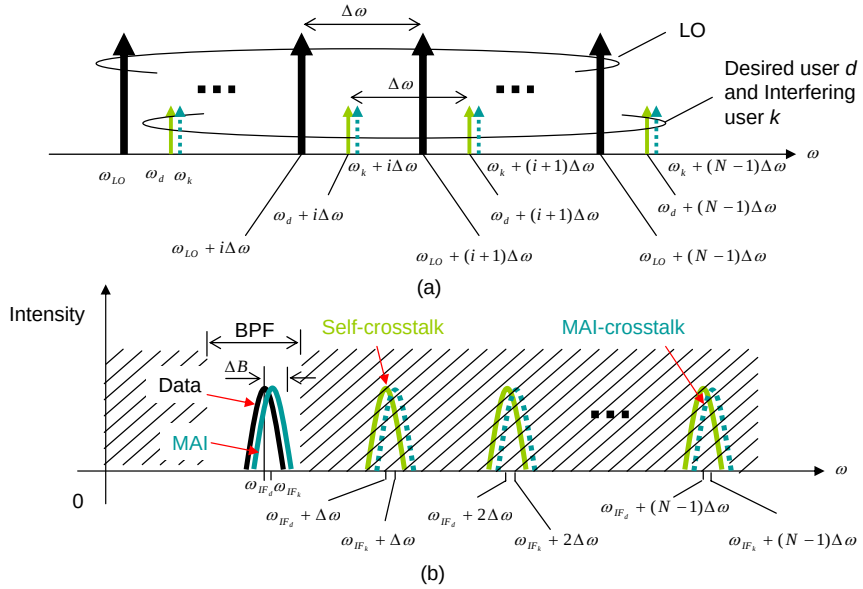

Fig. 4. (a) Optical spectra of the LO signal from desired user d and interfering user k . (b) Photodetected signal and passband of the BPF.

4. Numerical Results

In this section, numerical results are presented to highlight the advantages of the proposed system as well as the effect of the system parameters on its performance. We are interested in a broadband OMAN that supports 10 Gbit/s connections. For the analysis, we set up the system with 16, 32, and 48×10 Gbit/s users. Also, we used signature codes with a length of $N = 56$ and $B_{opt} = 1.28$ THz. Since Hadamard and m-sequence codes perform similarly, we analyzed only the former and apply the result for both. Hadamard and MQC code sets that have a length of $N = 56$ are (56, 28, 14) and (56, 8, 1), respectively.

Figure 5 shows the system's BER versus the effective optical power from user P_s when $P_{LO} = -10$ dBm and 1 dBm. The SAE/OCDM receiver sensitivity can be greatly improved even when the number of users increases. Moreover, for different numbers of users, 16, 32, and 48×10 Gbits/s, there is only a small difference (less than 0.5 dB) in the required optical power for the system to achieve BER $= 10^{-9}$ when P_{LO} is low (i.e., at -10 dBm). In addition, that difference no longer exists when $P_{LO} = 1$ dBm. Actually, at this relatively high P_{LO}, the number of users is limited by the signature code and encoder–decoder structure used. As shown in Fig. 5 with $P_{LO} = 1$ dBm, a BER of 10^{-9} can be achieved when $P_s = -44.5$ dBm regardless of the number of users (16, 32, or 48). This is due to the fact that the LO's shot noise becomes dominant when P_{LO} is high [see Eq. (13)].

Figure 6 shows the comparison between the performance of a SAE/OCDM system using Hadamard and MQC signature codes. Similar system parameters are used, and $P_{LO} =$ 1 dBm is set for $N = 48 \times 10$ Gbit/s users. Even if it is claimed that lower-weight codes (e.g., MQC codes) offer better performance in direct-detection systems (see Section 2), it is found that a higher-weight code (such as Hadamard or m-sequence code) is preferable in the heterodyne detection system. As a matter of fact, receiver sensitivity in the Hadamard coded system has an improvement of about 11 dB in the working range (i.e., BER $= 10^{-9}$) compared with the MQC coded system. This is because in the heterodyne detection system the effect of OBI, which is proportional to the square of the receiver's optical power, is

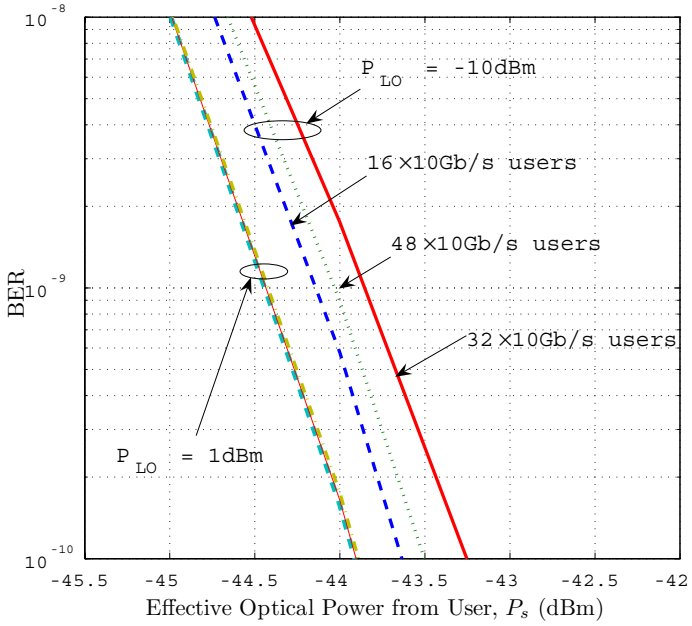

Fig. 5. BER versus effective optical power from user P_s (dBm). Synchronous detection, $P_{LO} = -10$ dBm. Hadamard code (56, 28, 14); number of users, $N = 16, 32, 48 \times 10$ Gbits/s; $B_{opt} = 1.28$ THz .

minor in comparison with the LO's shot noise. In this case, a higher-weight code, such as Hadamard code or *m*-sequence code, would result in a higher SNR.

Figure 6 also shows the performance of an asynchronous versus a synchronous heterodyne detection system. The asynchronous heterodyne detection system is seen to have only slightly worse performance than the synchronous one. The required power deference is less than 1 dB. This confirms that an asynchronous system is preferred thanks to its simplicity and easy implementation [12].

5. Conclusion

We have proposed a SAE/OCDM system with a heterodyne detection receiver. The system performance has been theoretically analyzed taking into account various types of noise and interference, such as MAI, OBI, cross talk, and receiver noise. Several signature codes have been considered, including *m*-sequence, Hadamard, and MQC signature codes. We noted that a heterodyne detection receiver can greatly improve the performance of a SAE/OCDM system. Numerical results show that 48×10 Gbit/s users can be supported at a received effective optical power of $P_s = -44.5$ dBm when $P_{LO} = 1$ dBm. Actually, when the LO's optical power is relatively high (e.g., 1 dBm in our analysis), the number of users is limited only by the code and encoder–decoder structure used. Moreover, it is found that signature codes with higher weight, such as Hadamard code and *m*-sequence code are preferable in a heterodyne detection system.

This paper has limitations, however. For the sake of analytical simplicity, we assumed ideal conditions. The effects of dispersion and polarization mismatch, which are critical issues in real systems, have not been taken into consideration. In our future research, we plan to study how to solve these issues.

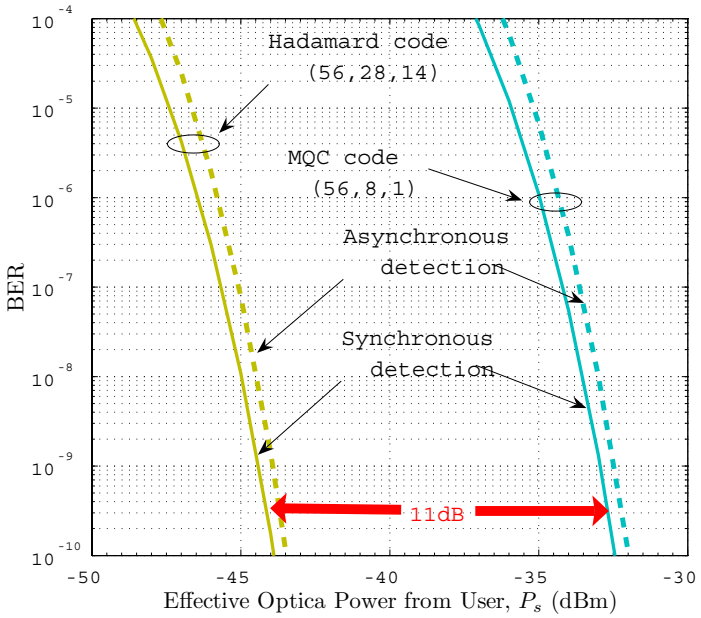

Fig. 6. BER versus effective optical power from user P_s (dBm). Hadamard code (56, 28, 14) versus MQC (56, 8, 1); synchronous detection versus asynchronous detection; number of users, $N = 48 \times 10\,\text{Gbits/s}$; $P_{LO} = 1\,\text{dBm}$; $B_{opt} = 1.28\,\text{THz}$.

Acknowledgments

The authors thank the reviewers for their thorough reviews and useful suggestions for improving the readability of this paper. This work was partly funded by Sasakawa Scientific Research Grant 17-074 from the Japan Science Society.

References and Links

[1] J. A. Salehi, A. M. Weiner, and J. P. Heritage, "Coherent ultrashort light pulse CDMA communication systems," J. Lightwave Technol. **8**, 478–491 (1990).

[2] Z. Jiang, D. Seo, S. Yang, D. E. Leaird, R. V. Roussev, C. Langrock, M. M. Fejer, and A. M. Weiner, "Four-user 10-Gb/s spectrally phase-coded O-CDMA system operating at 30 fJ/bit," IEEE Photon. Technol. Lett. **17**, 705–707 (2005).

[3] D. Zaccarin and M. Kavehrad, "An optical CDMA system based on spectral encoding of LED," IEEE Photon. Technol. Lett. **4**, 479–482, (1993).

[4] M. Kavehrad and D. Zaccarin, "Optical code-division-multiplexed systems based on spectral encoding of noncoherent sources," J. Lightwave Technol. **13**, 534–545 (1995).

[5] L. Nguyen, B. Aazhang, and J. F. Young, "All-optical CDMA with bipolar codes," Electron. Lett. **31**, 469–470 (1995).

[6] C. F. Lam, D. T. K. Tong, M. C. Wu, and E. Yablonovitch, "Experimental demonstration of bipolar optical CDMA system using a balanced transmitter and complementary spectral encoding," IEEE Photon. Technol. Lett. **10**, 1504–1506 (1998).

[7] E. D. J. Smith, P. T. Gough, and D. P. Taylor, "Noise limits of optical spectral-encoding CDMA systems," Electron. Lett. **31**, 1469–1470 (1995).

[8] X. Wang and K. Kitayama, "Analysis of beat noise in coherent and incoherent time-spreading OCDMA," J. Lightwave Technol. **22**, 2226–2232 (2004).

[9] E. D. J. Smith, R. J. Blaikie, and D. P. Taylor, "Performance enhancement of spectral-amplitude-coding optical CDMA using pulse-position modulation," IEEE Trans. Commun. **46**, 1176–1185 (1998).
[10] Z. Wei, H. M. H. Shalaby, and H. Ghafouri-Shiraz, "Modified quadratic congruence codes for fiber Bragg-grating-based spectral-amplitude-coding optical CDMA systems," J. Lightwave Technol. **19**, 1274–1281 (2001).
[11] Y. Maeda, K. Okada, and D. Faulkner, "FSAN OAN-WG and future issues for broadband optical access networks," IEEE Commun. Mag. **12**, 126–132 (2001).
[12] G. P. Agrawal, *Fiber-Optic Communication Systems*, 2nd ed. (Wiley-Interscience, 1997).
[13] J. Veselka and S. Korotky, "A multiwavelength source having precise channel spacing for WDM systems," IEEE Photon. Technol. Lett. **10**, 958–960 (1998).
[14] M. Fujiwara, J. Kani, H. Suzuki, K. Araya, and M. Teshima, "Flattened optical multicarrier generation of 12.5 GHz spaced 256 channels based on sinusoidal amplitude and phase hybrid modulation," Electron. Lett. **37**, 967–968 (2001).
[15] J. G. Proakis, *Digital Communications*, 4th ed. (McGraw-Hill, 2001).